(27) MID-SPAN DEBONDING STRENGTH MODEL FOR FRP STRENGTHENED RC BEAMS IN FLEXURE

Jianguo DAI[1], Hiroshi YOKOTA[2] and Tamon UEDA[3]

[1]Member of JSCE, Researcher, LCM Research Center, Port and Airport Reseach Institute
(Nagase 3-1-1, Yokosuka, 239-0826, Japan)
E-mail: dai@pari.go.jp
[2]Fellow of JSCE, Executive Researcher, Port and Airport Research Institute
(Nagase 3-1-1, Yokosuka, 239-0826, Japan)
E-mail: hiroy@pari.go.jp
[3]Member of JSCE, Professor, Division of Built Environment, Hokkaido University
(Kita 13 Nishi 8, Sapporo, 060-8628,. Japan)
E-mail: ueda@hokudai.ac.jp

This paper proposes a criterion to correlate mid-span debonding in FRP strengthened RC members to the yielding of internal steel reinforcement, which is an important mechanism inducing the debonding but can be assured for an appropriate ultimate state design. Through analysis, this paper concluded that the mid-span debonding in FRP strengthened RC members can be simply attributed to the formulation of a critical steel yielding length, beyond which the gradient of the tensile force in FRP exceeds its threshold value. The new debonding criterion is based on traditional sectional analysis hence complex bond stress-slip analysis can be avoided. Further, it can incorporate the bond properties of FRP/concrete interfaces, beam geometries, and properties of reinforcement and FRP in the mid-span debonding strength analysis. Based upon a solid database, the simple criterion demonstrated its validity.

Key Words *fiber reinforced plastics, RC beams, strengthening, yielding zone, bond strength, debonding*

1. INTRODUCTION

Using externally bonded FRP sheets/laminates to strengthen reinforced concrete (RC) beams in flexure has gained worldwide popularity. However, a major concern for FRP flexural strengthening is the premature debonding between FRP and concrete substrate since the bonding interface proves to be the weakest link in the whole strengthening system. As has been well documented (Buyukozturk and Hearing 1998; Triantafillou 1999; Sebastian 2001; Teng et al. 2002; Oehlers 2005), two major debonding mechanisms have been widely observed. One is the plate-end debonding initiating from the termination point of FRP. The main factors causing this failure are understood to be the distance between the termination positions of the FRP and the beam supports and the use of thick FRP plates. In practice, this failure can be avoided by extending the FRP as near as possible to the beam supports or by installing U-shape anchorage systems at the FRP ends. Another is the mid-span debonding (also popularly called intermediate crack-induced debonding) that is caused by the opening of major flexural and flexure-shear cracks (Teng et al. 2003). Since the mid-span debonding is the most prevalent failure mode in FRP strengthened RC flexural members, design codes (ACI 440, 2002, FIB 2001, JSCE 2001) have specified methods to predict the member strength corresponding to this failure mode. Recently, further efforts have been put into predicting the full-range debonding processes along the cracked concrete beams with the uses of crack spacing and bond-slip behavior of FRP/concrete interfaces. Models recently developed for predicting the mid-span debonding in FRP strengthened flexural RC members can be mainly sorted into the following two types:

(1) Strain limit-based approach. The concept for this approach is to limit the strain/stress in the externally bonded FRP to a certain level. In the FIB 2001 code, the strain in FRP is limited to less than five times the

steel yielding strain and half of the characteristic values of the ultimate strain of the FRP according to the manufactures. The ACI 440 (2002) code correlates this strain limit to the tension stiffness of FRP. Forthcoming revisions of the ACI 440 code adopt the Teng et al. (2003) approach to addressing debonding although with different calibration factors. The debonding strain in FRP has also been correlated with other factors like the fracture energy of FRP/concrete interface (JSCE 2001), concrete strength, the ratio of FRP width to concrete surface width (Teng et al. 2003), bond length of FRP, the effective bond length of FRP/concrete interface, and the maximum interfacial bond stress (Lu et al. 2007). These strain limit models derived from various approaches are preferred in practical design. But their reliability is questioned since they reflect the influences of FRP properties and the interface bond while generally neglecting information of beam geometries and internal reinforcement ratio.

(2) Stress variation-based approach. In this approach, the distribution of cracks in FRP strengthened flexural RC beams needs to be considered and the bond stress-slip relationship for the FRP sheet/concrete interface is necessary to be implemented for an analysis. For strengthened members with a single flexural crack, the debonding strength analysis is not complex. The debonding stress in FRP can be determined using Mode II fracture energy of FRP/concrete interfaces (Holzenkämpfer 1994; Täljsten 1996; Brosens and Van Germert 1998). For practical cases in which multiple cracks exist in the FRP strengthened RC members, the mid-span debonding failure needs to be predicted considering the variation of tensile stresses in the FRP bonded with a concrete block between two adjacent cracks. Early analytical work related to this debonding mechanism can be found in the work by Niedermeier (2000) and Niu and Wu (2001, 2002), which was reflected in FIB (2001) and JSCE codes (2001), respectively. Recently, continuing efforts are put into clarifying the full-stage variation of tensile stresses in FRP that bridges multiple cracks based on a local deformation model (Smith and Gravina 2007), partial interaction theory (Liu et al. 2007), discrete FEM modeling (Niu and Wu 2006), and closed-form solutions (Chen et al. 2005; Ibars 2005; Pan and Leung 2005; Teng et al. 2006) using bilinear or tri-linear interfacial bond stress-slip models.

These stress variation-based approaches are more generic and believed to be superior to existing strain-limit models because they help us understand quantitatively the effects of number of cracks, beam geometry, and interface bond properties on whole-stage interface debonding process. However, their complexity is an impediment to developing a practical debonding strength model that can unify all the design parameters. Also, most of these stress variation-based models are very sensitive to the determination of crack-spacing, for which no good models have been proposed for FRP strengthened RC members. One more issue remaining theoretically controversial is that the debonding strains of FRP are derived from complex bond-slip analysis in these models and the loss of partial or whole bond actions between FRP and one or more cracked concrete blocks is allowed at the ultimate state. These derived local strains in FRP may better reflect reality. However, when meant for practical design, for which the conventional compatibility analysis neglecting the slip between the FRP and concrete is usually applied, their applicability requires further confirmation.

This paper proposes a simple criterion for predicting the mid-span debonding strength of FRP strengthened flexural RC beams using the steel yielding phenomenon. Using this simple but useful criterion, all the geometrical information of strengthened RC beams, reinforcement details, and the bond properties of FRP/concrete interfaces can be incooperated in the mid-span debonding strength analysis while avoiding complex bond stress-slip analysis and the use of other controversial parameters such as crack spacing, effective bond length etc.

2. CRITICAL STEEL YIELDING LENGTH IN FRP STREGNTHENED RC MEMBERS

Failure in FRP strengthened flexural RC members can be classified into five modes (JSCE 2001): (1) FRP fracturing after steel yields; (2) Concrete crushing after steel yields; (3) Concrete crushing before steel yields; (4) Debonding of FRP at the anchorage zone; and (5) Mid-span debonding. A conventional compatibility approach can be employed for analyzing the failure mechanisms of Mode (1) - (3). Mode (4) is related to the stress concentration at the termination point of FRP and is beyond the scope of this paper. Mode (5) is the most prevalent failure mode in FRP strengthened RC beams and is considered in this paper.

Considering a FRP strengthened RC beam under three-point bending as an example (see **Fig.1**), different from a FRP/concrete joint under simple shear, a FRP strengthened RC beam under flexure has two important mechanisms influencing the mid-span debonding between FRP and concrete. One is the influence of multiple cracks, which has been pointed out by many researchers as reviewed in the previous section. It can be seen from **Fig.1** that the existence of cracks causes variations of tensile forces in both FRP and steel reinforcement at cracked and un-cracked sections because of the well-known tension stiffening affect through the bond between concrete and steel and FRP. Obviously, good understanding on the local bond stress-slip models for FRP/concrete interfaces helps us to predict these variations and to understand the whole interface debonding process. However, conceptually it should be kept in mind that the critical mechanism to cause the macro-debonding failure of an FRP strengthened system still is the critical gradient of tensile force in FRP in the shear span (see **Fig.1**), implying a similar debonding nature in the flexural test and simple shear test.

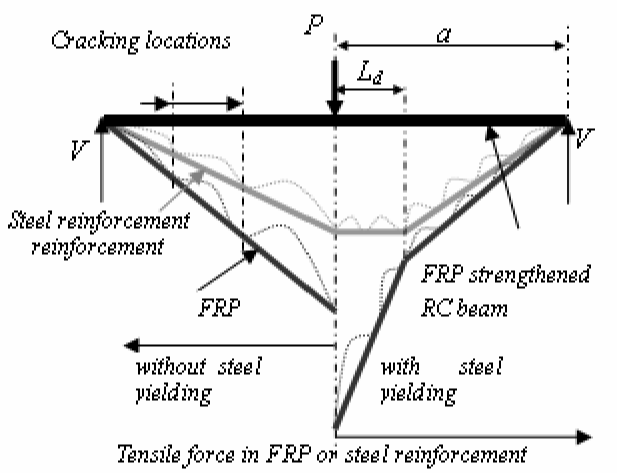

Fig. 1 Difference in tensile stress profile in FRP before and after steel yields

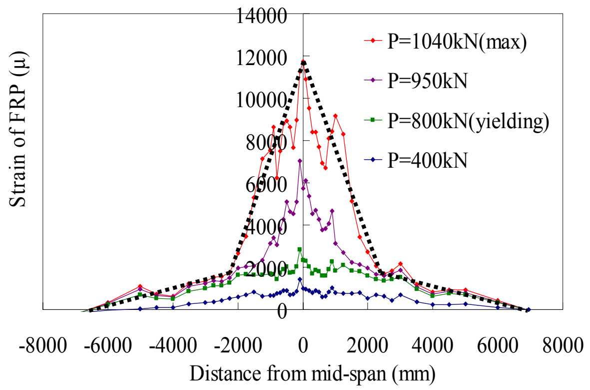

Fig.2 Strain profiles of FRP in a large-span RC deck strengthened with FRP(Dai et al. 2005a)

Steel yielding is another important mechanism influencing the mid-span debonding but has only received limited attention in the past (Ibars 2005; Wu and Niu 2007). As shown in **Fig.1**, the tensile force profiles in FRP in the shear span change dramatically before and after steel yielding. This phenomenon is especially easy to observe in large-scale specimens. **Fig.2** presents the strain profiles in the FRP for the strengthening of a bridge deck with a large span (Dai et al. 2005a). It can be clearly seen that the strain gradients in FRP behave differently in and out of the steel yielding zone after steel yields. Similar strain profiles of FRP within the steel yielding zone can be found in the FEM analytical results by Niu and Wu (2001) and Lu et al. (2007). Obviously, the yielding of steel reinforcement not only leads to an increase of local strain in FRP but also leads to an increase of the local strain gradient in FRP. In practice, most FRP strengthened RC beams are designed with steel yielding at the ultimate state. Hence great interest remains in the possibility of building a direct relationship between the steel yielding and the ultimate mid-span debonding while avoiding complex analyses based on crack distribution and interfacial bond-slip relationships.

For a simply-supported FRP strengthened RC beam with steel yielding as seen in Fig.1, conceptually there is a relationship between the steel yielding length and the ultimate sectional moment as follows:

$$L_{y,u} = (M_u - M_y)/V_u = (1 - M_y/M_u)\cdot a \quad (1)$$

where $L_{y,\ u}$ = the steel yielding length in the strengthened member at the ultimate state; M_u = maximum moment capacity of the strengthened RC member; M_y = maximum moment in the member at initial steel yielding; V_u = shear force in the member at the ultimate state; a = shear span.

From **Eq.1** it can be seen that the steel yielding length can be a parameter to bridge the ultimate member strength with the beam geometry; such as the shear span and the beam's sectional information including beam depth and reinforcing ratio etc. Naturally, for those FRP strengthened RC beams with debonding failure after the steel yielding, the debonding strength can be predicted once the length of steel yielding zone at debonding is known.

3. TENSILE FORCE VARIATIONS IN FRP DRIVEN BY STEEL YIELDING

Traditional moment-curvature analysis based on plane section assumption has proved to be applicable for predicting the behavior of FRP strengthened RC beams (Saadatmanesh and Ehsani 1991). So it is not difficult to obtain the tensile force in FRP in the beam section with initial steel yielding. Once the gradient of the tensile force in the FRP, in other words, the average bond stress of FRP/concrete interface within the steel yielding zone is known, the tensile force in FRP at the section with the maximum moment can be obtained as follows:

$$\sigma_{u,frp} = \sigma_{y,frp} + \tau_{aver,u} L_{y.u} / t_{frp} \quad (2)$$

where $\sigma_{u,frp}$= the maximum tensile force in FRP at the ultimate state; $\sigma_{y,frp}$ = the tensile force in FRP at the beam section with initial steel yielding; $\tau_{aver,u}$ = the average bond stress in the FRP/concrete interface within the steel yielding zone; t_{frp} = the thickness of FRP.

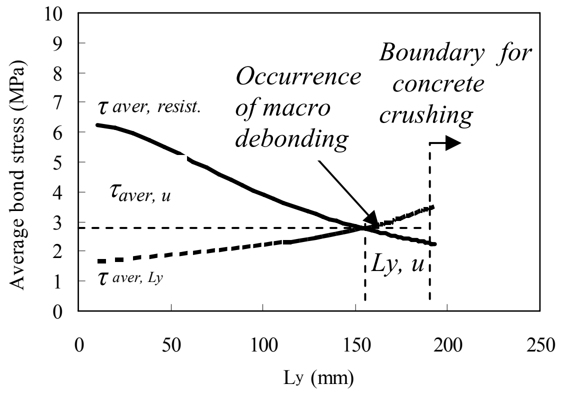

Fig. 3 Typical relationship between the average bond stress in FRP/concrete interface within the yielding zone and the steel yielding length

The dotted line in **Fig.3** shows a typical relationship between the average bond stress $\tau_{aver,Ly}$ in the FRP/concrete interface within the steel yielding zone and the steel yielding length L_y, which can be obtained through a traditional sectional analysis. It can be seen that $\tau_{aver,Ly}$ driven by the steel yielding always increases with the steel yielding length L_y. Therefore, the occurrence of mid-span debonding can be attributed to the average bond stress in the steel yielding zone reaching a threshold value beyond which the yielding length can not increase. This threshold value is related to the bond resistance of FRP /concrete interface under shear because, as mentioned above, shear is the mechanism causing the gradient of the tensile force in the FRP. It should also be noticed that concrete crushing, instead of the mid-span debonding, will occur if the average bond stress within the yielding zone never reaches its threshold value before the top concrete fiber reaches its ultimate strain capacity.

4. BOND RESISTANCE OF FRP/CONCRETE INTERFACE UNDER SIMPLE SHEAR

Theoretically, for a FRP/concrete joint with a sufficiently long bond length under simple shear (see **Fig. 4**), the maximum tensile force achieved in FRP can be expressed as (Dai et al. 2005b):

$$P_{\max} = b_f \sqrt{2E_f t_f G_f} \quad (3)$$

where G_f = is the interfacial fracture energy; E_f, t_f = the elastic modulus and thickness of the FRP, respectively; b_f = the width of FRP. Dai et al (2005b) also proposed a local bond stress-slip relationship for the FRP/concrete interface as follows:

$$\tau = 2BG_f(\exp(-Bs) - \exp(-2Bs)) \quad (4)$$

where τ = local interfacial bond stress; s = local interfacial slip; B = interfacial ductility factor. The interfacial fracture energy G_f and B were found to change greatly when using softer non-linear adhesives (Dai et al. 2005b). For popularly used linear bonding adhesives, Dai et al. (2006) suggests taking the values of G_f and B based on regression analysis of many test results as follows:

$$G_f = 0.514 f_c'^{0.236} \quad (5)$$

$$B = 10.4 \quad (6)$$

Once the interfacial bond-stress slip relationship is known, it is possible to predict the full-range shear bond stress distribution in the FRP/concrete interface under simple shear (see **Fig. 4**). Using this bond stress distribution, it is also possible to predict the maximum gradient of tensile force in FRP that can be achieved over a given bond length of L_b (see **Fig.4**) using the following formulation (Dai et al. 2006):

$$\Delta P_{\max,L_d} = \alpha P_{\max} \quad (7)$$

$$\alpha = (e^{\beta} - 1)/(e^{\beta} + 1) \quad (8)$$

$$\beta = L_b B \sqrt{G_f} \Big/ \sqrt{2E_f t_f} \quad (9)$$

where $\Delta P_{max,Ld}$ = the maximum gradient of tensile force that can be achieved in a bond area with the length L_b. As a consequence, the average bond stress resistance $\tau_{aver,resist.}(L_b)$ over a given bond length L_b can be formulated as follows:

$$\begin{aligned}\tau_{aver,resist}(L_b) &= \Delta P_{\max,L_d} \big/ (b_f L_b) \\ &= \alpha\sqrt{2G_f E_f t_f}\end{aligned} \quad (10)$$

If the relationship between $\tau_{aver,resist}(L_b)$ and L_b is plotted in **Fig.3**, it is seen that $\tau_{aver,resist}$ decreases with the increase of L_d. When L_b approaches 0, mathematically **Eq. 10** will converge to the value equal to $0.5G_fB$, whose physical meaning is the maximum local bond stress in the local bond stress-slip relationship (Dai et al 2005b).

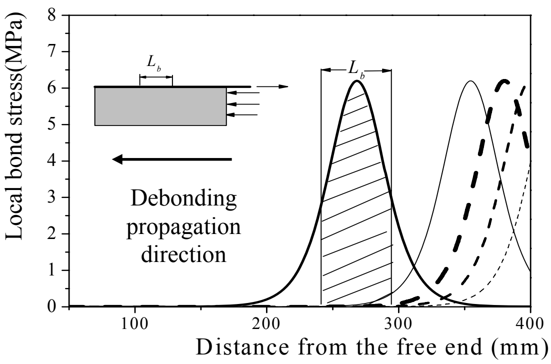

Fig. 4 Typical shear bond stress distribution in FRP/concrete joints under a simple shear test

5. NEW MID-SPAN DEBONDING CRITERION AND VERIFICATION

Accepting that the primary mechanism leading to the macro-debonding is the shear-induced tensile force gradient in the FRP, it is interesting to see the relationship between the threshold average bond stress within the steel yielding zone and the average bond resistance of a FRP/concrete interface under simple shear. For this purpose, conventional moment-curvature analysis was performed for FRP strengthened RC members based on a database of 97 tests chosen from 17 sources. To have reliable analyses and to acheive the purposes of the current study, the following criteria were applied for selecting test results from the available literature.

(1) All beam geometry information including beam height and width, shear span, effective depth and cover depth are available;

(2) All the reinforcing information including the reinforcing ratio, elastic modulus and yield strength of steel reinforcement, and the elastic modulus, bond width, and thickness of FRP materials was available;

(3) No shear failure was reported for the selected beams/slabs. Also, for the selected beams/slabs, the distance between the FRP termination point and the support was sufficiently short to avoid plate-end effects. For this purpose, it was required that the FRP length within the shear span was more than 90% of the shear span; and

(4) In the literatures, some beams/slabs were reported to have debonding failure. But if they had reported debonding strengths larger than the analytical member strengths corresponding to a concrete crushing failure, they were removed from the database because this condition was unreasonable in reality if all the material properties, such as the mechanical properties of FRP and concrete, were correctly reported. **Table 1** presents a summary of the range of material and geometry properties of the eventually selected beams/slabs.

An analysis was performed for each FRP strengthened member based on strain compatibility and force equilibrium (see **Fig.5**) conditions. The plane sections assumption was applied and no slip was assumed between FRP and concrete. An elastic-perfectly plastic relationship was assumed for the steel reinforcement and a linear relationship was assumed for the FRP to fracture. Hognestad's parabolic stress-strain model was used to describe the constitutive law for concrete in compression (see **Fig. 6**). The detailed analytical procedures for each strengthened member were as follows:

(1) Calculate the initial yielding moment M_y and the corresponding tensile stress $\sigma_{y,frp}$ in the FRP. Since the experimental maximum moment was known, the steel yielding length $L_{y,u}$ at the ultimate state is calculated using **Eq. 1**. The maximum tensile stress $\sigma_{u,frp}$ in the FRP at the ultimate state is also obtained;

(2) Using **Eq. 2,** the average bond stress $\tau_{aver,u}$ within the steel yielding zone is calculated; and

(3) Using **Eq. 9,** the average bond stress resistance $\tau_{\mathrm{aver,\ resist}}$ over a given bond length L_y under simple shear is determined.

Figure 7 shows the comparison between $\tau_{aver,u}$ and $\tau_{aver,resist.}$ It is interesting to find that the two values show clear consistentency in spite of the observed scatter. The degree of scatter was understandable because the scatter of the bond strength of the FRP/concrete interface is very large.

As reported by Ueda and Dai (2005), the interfacial fracture energy was found to vary from 0.5 to 2.5N/mm based on the investigation of 231 shear tests of FRP/concrete bonded joints. As discussed in the previous section, the average bond stress in the FRP/concrete interface increases with the steel yielding length and reaches a threshold value at the ultimate state. Through the current analysis and comparison, it appears that this threshold value can be predicted using the presented bond model (**Eq. 9**). Therefore, a criterion is proposed in **Fig. 3** to predict the maximum steel yielding length corresponding to the mid-span debonding strength. Since the average bond stress driven by the steel yielding zone increases while the average bond stress resistance decreases with the increase of steel yielding length, there is a point where the values reach the same value indicating the occurrence of macro debonding (see **Fig.3**). In other words, the debonding criterion can be formulated as follows:

$$\tau_{aver,u} = \tau_{aver,resist.}(L_{y,u}) \qquad (11)$$

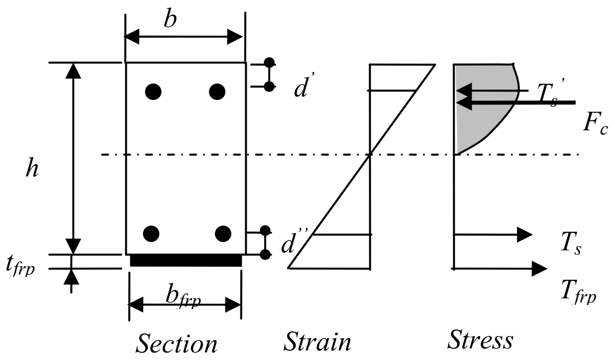

Fig. 5 Stress and strain profiles of FRP strengthened cross section

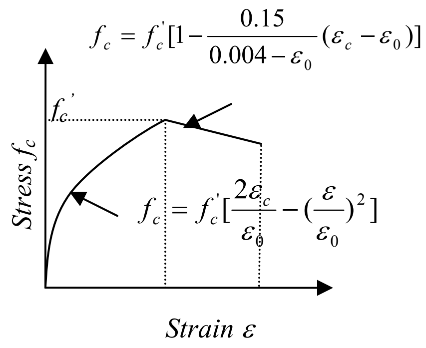

Fig.6 Hognestad's concrete model

If the two curves never intersect, concrete crushing will occur instead of mid-span debonding (see **Fig. 3**). The proposed criterion indicates that the occurrence of mid-span debonding can be attributed to the formulation of a critical debonding zone, where the tensile stress gradient of the FRP reaches its threshold value. For FRP strengthened RC beams with steel yielding, the critical bond length seems to be equivalent to the steel yielding length at the ultimate state. Moreover, the threshold gradient of tensile stress in the FRP proves to be equivalent in flexural tests of FRP strengthened RC beams and simple shear tests of FRP/concrete joints. Therefore, for FRP stregnthed RC members with flexural yielding, the existence of multiple cracks seems not to have a significant influence on the critical tensileforce gradient of the FRP but on the maximum tensile force in FRP. For FRP strengthened RC beams without steel yielding or FRP strengthened plain concrete beams, the overall gradient of tensile force in the FRP can be treated as a constant value (see **Fig. 3**). Therefore once the average bond stress in the FRP/concrete interface within any a critical bond length reaches the threshold value, mid-span debonding will occur. However the issue of how to determine the critical bond length remains for further study. Smith and Gravina (2005) proposed a critical bond length equal to one or two times the effective length of FRP/concrete joints under simple shear tests. The reliability of this definition must be verified based on more data accumulation since there are very few test data available for FRP strengthened RC beams without steel yielding or for FRP strengthened plain concrete beams with multiple cracks. But on the other hand, both cases rarely appear in a practical design.

Figure 8 presents comparisons between the analytical and experimental results in terms of ultimate loading carrying capacity. The maximum, minimum, and average ratios of predicted debonding strengths to experimental capacity are 1.22, 0.81, and 0.99, respectively, and the coefficient of variation is 0.1, indicating the validity of the proposed mid-span debonding criterion.

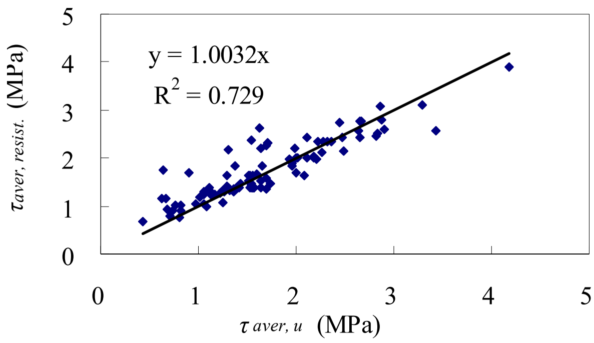

Fig.7 Comparison between $\tau_{aver, u}$ and $\tau_{aver, resist.}$

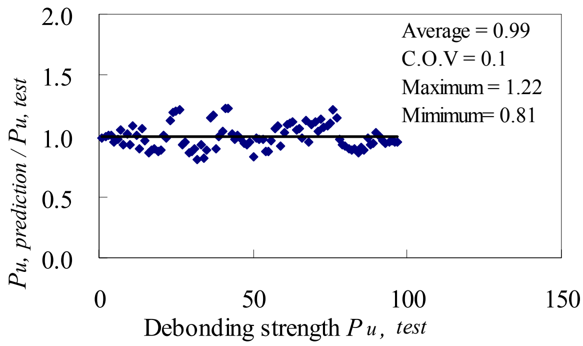

Fig.8 Comparison between predicted and experimental load-carrying capacity

ACKNOWLEDGEMENT The authors would like to thank Prof Zhishen WU, Ibaraki University for his providing database for the analysis in this paper, and Dr H Kent A. Harries, University of Pittsburgh, U.S.A, for his valuable communications on the paper.

6. CONCLUSIONS

Steel yielding is an important mechanism influencing the mid-span debonding in FRP strengthened RC members. A simple criterion has been proposed for predicting mid-span debonding failure in FRP strengthened flexural RC members with steel yielding, which is required in an appropriate ultimate state design. In this criterion mid-span debonding has been attributed to the formulation of a threshold gradient of tensile force in the FRP within a critical bond zone rather than an arbitrary tensile force in FRP. The critical bond zone proves to be equivalent to the length of steel yielding in FRP strengthened flexural RC members with steel yielding. Based on analysis of a database including 97 tests, the threshold gradient of tensile force in FRP within the critical bond zone proves to be equivalent in flexural tests of FRP strengthened RC beams and in simple shear tests of FRP/concrete joints. The proposed mid-span debonding criterion is believed to be a simple but useful tool to incorporate the effects of beam geometry, internal reinforcing and external strengthening information, and the bond properties of FRP/concrete interfaces in a mid-span debonding analysis. Each parameter used has clear physical meaning. Moreover, complex bond stress -slip analyses can be avoided since a conventional compatibility analysis based on the plane sections assumption is applicable for the analysis.

REFERENCES

ACI 440. 2R-02 (2002), ‘‘Guide for the design and construction of externally bonded FRP systems for strengthening concrete structures.’’

Beber, A. J., Campos Filho, A., Campagnolo, J. L.: Flexural strengthening of R/C beams with CFRP sheets, Proceedings of 8th International Structural Faults and Repair Conference, London, 1999.

Brosens, K. and Van Gemert, D. (1998), “Plate end shear design for external CFRP laminates”, *Proceedings of FRAMCOS-3*, Aedificatio Publishers, Freiburg, Germany, 1793-1804.

Buyukozturk O., and Hearing B. (1998), ‘‘Fracture behavior of precracked concrete beams retrofitting with FRP.’’ *J. Compos. Constr.,* 2(3), 138-144.

Chan, T. K., Li, X. A. (2000), ‘‘Improving crack behavior of one-way slabs with carbon fibre plates.’’ *Proceedings of the 4-th Asia Pacific Structural Engineering & Construction Conference*, Kuala Lumpur, Malaysia, 351-358.

Chen, J.F., Yuan, H. and Teng, J. G. (2005), ‘‘Analysis of debonding failure along a softening FRP-to-concrete interface between two adjacent cracks.’’ *Proceedings of the International Symposium on Bond Behavior of FRP in Structures (BBFS 2005)*, Chen and Teng (eds), 103-112.

Dai, J. G., Ueda, T., Sato, Y. and Ito, Y. (2005a), ‘‘Flexural strengthening of RC beams using externally bonded FRP sheets through flexible adhesive bonding.’’ *Proceedings of the International Symposium on Bond Behavior of FRP in Structures (BBFS 2005)*, Chen and Teng (eds), 213-222.

Dai, J. G., Ueda, T. and Sato, Y. (2005b), ‘‘Development of nonlinear bond stress-slip model of FRP sheet-concrete interfaces with a simple method.’’ *J. Compos. Constr.,* 9(1), 52-62.

Dai, J. G., Ueda, T. and Sato, Y. (2006), ‘‘Unified analytical approaches for determining shear bond characteristics of FRP-concrete interfaces through pullout tests.’’ *Journal of Advanced Concrete Technology,* 4(1), 133-145.

Delaney, J. (2006), ‘‘Defect criticality of FRP rehabilitated RC beams.’’ Master’s thesis, University of California, San Diego.

FIB. (2001), ‘‘Externally bonded FRP reinforcement for RC structures.’’ Bulletin 14, Lausanne, Switzerland.

Garden, H. N., Quantrill, R. J., Hollaway, L. C., Thorne, A. M., Parke, G. A. R. (1998), ‘‘An experimental study of the anchorage length of carbon fiber composite plates used to strengthen reinforced concrete beams.’’ *Constru. Building. Mater.*, 12, 203-219.

Holzenkämfer, O. (1994), ‘‘*Ingenieurmodelle des Verbundes geklebter Bewehrung für Betonbauteile*.’’ Dissertation, TU Braunschweig, Germany.

Ibars, E. O. (2005), ‘‘*Peeling failure in beams strengthened by plate bonding: A design proposal.*’’*, Ph. D* dissertation submitted to Department d’Enginyeria de la Construcció, Universitat Politècnica de Catalunya.

JSCE. (2001), ‘‘Recommendations for upgrading of concrete structures with use of continuous fiber sheets.’’*Concrete Engineering Series 41*, Japan Society of Civil Engineers.

Kishi, N., Mikami, H., Sato, M., Matsoka, K. (1998), ‘‘Flexural bond behavior of RC beams externally bonded with FRP sheets.’’ *Proceedings of the Japan Concrete Institute,* 20(1), 515-520.

Kishi, N., Mikami, H., Zhang, G. (2003), ‘‘Numerical analysis of debonding behavior of FRP sheet for flexural strengthening RC beams.’’ *Journal of Materials, Concrete Structures and Pavements*, No. 58, No. 725, pp. 255-272.

Kurihashi, Y., Kishi, N., Mikami, H., Matsoka, K. (2000), ‘‘Effect of FRP reinforcement amount on flexural bond behavior of FRP-strengthened RC beams.’’ *Proceedings of the Japan Concrete Institute*, 22(1), 481-486.

Kotynia, R. (2005), ‘‘Debonding failures of RC beams strengthened with externally bonded strips.’’ *Proceedings of the International Symposium on Bond Behaviour of FRP in Structures (BBFS 2005)*, Chen and Teng (eds), 247-252.

Liu, I.S.T., Oehlers, D.J. and Seracino, R. (2007), ‘‘Study of intermediate crack debonding in adhesively plated beams’’, *J. Compos. Constr.,* 11(2), 175-183.

Liu, I. S. T., Oehlers, D. J. and Seracino, R.(2007), ‘‘Study of intermediate crack debonding in adhesively plated beams.’’, *J. Compos. Constr.,* 11(2), 175-183.

Lu, X. Z., Teng, J.G., Ye, L.P. and Jiang, J. J. (2007). ‘‘Intermediate crack debonding in FRP-strengthened beams: FE analysis and strength model.’’ *J. Compos. Constr.,* 11(2), 161-174.

Oehlers, D.J. (2005). “Generic Debonding Mechanisms in FRP Plated Beams and Slabs.” *International Symposium on Bond Behaviour in FRP Structures*, Chen and Teng ediors. Hong Kong, December 2005, 35-44.

Saadatmanesh, H., and Ehsani, M. R. (1991). ‘‘RC beams strengthened with GFRP plates. I: Experimental study.’’ *J. Struct. Eng.,*117(11), 3417-3433.

Niedermeier R. (2000), ‘‘Zugkraftdeckung bei klebearmierten bauteilen (Envelope line of tensile forces while using externally bonded reinforcement)’’, in TU Munchen (in German)

Niu, H. and Wu, Z. S. (2001), ‘‘Interfacial debonding mechanism influenced by flexural cracks in FRP-strengthened beams.’’ *J. Struct. Eng., JSCE*, 47A, 1277-1288

Niu, H. and Wu, Z. S. (2002), ‘‘Strengthening effects of RC flexural members with FRP sheets affected by adhesive layers.’’ *Journal of Applied Mechanics*, 5, 887-897.

Niu, H. D. and Wu, Z. S. (2006), ‘‘Numerical analysis of debonding mechanisms of FRP-strengthened reinforced concrete beams.’’ *Computer-aided civil and infrastructure* *engineering*, 20(5), 354-3687.

Pan, J. W and Leung, C. K. Y. (2005), ''FRP debonding under the presence of multiple cracks along a concrete beam'', *Proceedings of the International Symposium on Bond Behavior of FRP in Structures (BBFS 2005)*, Chen and Teng (eds), 299-304.

Rahimi, H., Hutchinson, A. (2001), ''Concrete beams strengthened with externally bonded FRP plates'', *J. Compos. Constr.*, 5（1）, . 44-56.

Seim, W., Hörmann, M., Karbhari, V., and Seible, F. (2001), ''External FRP poststrengthening of scaled concrete slabs.'' *J. Compos. Constr.*, 5(2), 67-75.

Spadea, G., Swamy, R. N., Bencardino, F. (2001), ''Strength and ductility of RC beams repaired with bonded CFRP laminates.'' *Journal of Bridge Engineering*, 6(5), 345-355.

Sebastian W. M. (2001), ''Significance of midspan debonding failure in FRP-plated concrete beams.'' *J. Struct Eng.*, 127(7), 792-798.

Smith, Scott. T. and Gravina, Rebecca J. (2007), ''Modeling debonding failure in FRP flexurally strengthened RC members using a local deformation model.'' *J. Compos. Constr.,* 11(2), 184-191.

Takeo, K., Matsushita, H., Sagawa, Y., Ushigome, T. (1999), Experiment of RC beam reinforced with CFRP adhesive method having variety of shear-span ratio, *Proceedings of the Japan Concrete Institute*, 21(2), 205-210.

Täljsten, B. (1996), ''Strengthening of concrete prism using the plate-bonding technique'', *International Journal of Fracture*, V. 81, 253-266.

Teng, J. G.; Yuan, H.; Chen, J. F. (2006); ''FRP-to-concrete interfaces between two adjacent cracks : Theoretical model for debonding failure.'' *International journal of solids and structures*, 43(18-19), 5750-5778.

Teng, J. G., Chen, J. F., Smith, S. T., and Lam, L. (2002), ''*FRP Strengthened RC Structures*'', Wiley, West Sussex, U.K.

Teng, J.G., Smith, S. T., Yao, J., and Chen, J. F. (2003). ''Intermediate crack-induced debonding in RC beams and slabs.'' *Constru. Building. Mater.,* 17(6-7), 447-462.

Triantafillou T. C. (1999), ''*Guidelines for the Dimensioning of Reinforced Concrete Elements Strengthened with Sika Carbondur/Sikawrap.*'' University of Patras, Greece.

Ueda, T. and Dai, J. (2005), ''Mode II Fracture Energy of FRP-Concrete Interfaces: its evaluation and roles in interface modeling and anchorage design'', *Proceedings of the 11th International Conference on Fracture*, Paper No.4302 (CD-ROM), Turin, Italy.

Wu, Z. S. and Niu, H. D. (2007), ''Prediction of crack-induced debonding failure in R/C Structures flexurally strengthened with externally bonded FRP composites.'', *Journal of Materials, Concrete Structures and Pavements* (in press).

Yao, J.; Teng, J.G.; Lam, L. (2005), ''Experimental study on intermediate crack debonding in FRP-Strengthened RC flexural members.'' *Advances in Structural Engineering,* 8(4), 365-396.

Zarniç, R., Gostic, S., Bosiljkov, V., Bokan-Bosiljkov, V. (1999), ''Improvement of bending load-bearing capacity by externally bonded plates.'' *Proceedings of Creating with Concrete,* Dhir and Henderson (eds), London, Thomas Telford, 433-442.

Zhang, G. F., Kishi, N., Mikami, H., and Komuro, M. (2005), ''a numerical prediction method for flexural behavior of RC beams reinforced with FRP sheet.'' *Proceedings of the International Symposium on Bond Behaviour of FRP in Structures (BBFS 2005),* Chen and Teng (eds), 215-220.

(Received September 10, 2007)

Table 1 Summary of material and geometry properties of selected beams/slabs

Test variables	Specimen parameter	Maximum	Minimum	Average
Beam/slab geometry	Depth $h(mm)$	470	100	243
	Width $b(mm)$	800	100	200
	Shear span $a(mm)$	1982.5	340	1024
	Cover depth d'' (mm)	65	15	36
	Shear span/depth ratio a/d	10	2.1	4.7
Tensile reinforcement	Elastic modulus $Es(GPa)$	220	190	206
	Reinforcing ratio ρ_S (%)	1.14	0.33	0.73
	Yielding strength $f_{y,s}$ (MPa)	565	256	406
FRP Strengthening ratio	Elastic modulus (GPa)	271	20.5	173
	Thickness t_{frp} (mm)	6	0.71	0.71
	Tension stiffness $E_{frp}t_{frp}(N/mm)$	308	17.5	99.5
	Width b_{frp} (mm)	200	30	117
	Tensile strength $f_{frp,u}$ (MPa)	4519	269	2742
	Bond length in shear span l_a (mm)	1827.5	320	944.6
	l_a/a	9.95	2.21	4.65
	Strengthening ratio $E_{frp}b_{frp}t_{frp}/(E_sA_s)$	0.69	0.03	0.19
Concrete	Compressive strength f_c' (MPa)	60.8	12.6	33.2

Note: the database of 96 tests for the current analysis was from Saadatmanesh and Ehsani(1991), Garden et al.(1998), Kishi et al. (1998, 2003), Beber et al. (1999), Takeo et al.(1999), Chan and Li (2000), Kurihashi et al.(2000), Rahimi and Hutchinson(2001), Seim et al.(2001), Spadea et al.(2001), Dai et al. (2005), Kotynia(2005), Yao et al.(2005), Zarnic et al.(1999), Zhang et al.(2005), and Delaney (2006)